Milling Performance of C_f/SiC Composites: Three-Dimensional Finite Element Analysis and Experimental Validation

ELLAHI Zohaib, ZHAO Guolong*, NIAN Zhiwen, MUHAMMAD Jamil, HE Ning

College of Mechanical and Electrical Engineering，Nanjing University of Aeronautics and Astronautics，
Nanjing 210016，P. R. China

Abstract: Carbon fiber reinforced silicon carbide （C_f/SiC） composite materials possess high strength, wear resistance, and anisotropy, thus their machining is very difficult and demands extra precautions. In this research, finite element analysis （FEA） simulations and experiments of the slot milling process have been carried out to analyze the cutting performance of C_f/SiC with a polycrystalline diamond （PCD） tool. Effects of machining parameters on cutting forces are studied and material removal mechanisms at different fiber cutting angles have been investigated. The finite element model has been generated in ABAQUS/CAE software and the machining is performed. by using user-defined material subroutine. Effects of machining parameters on cutting forces are calculated through FEA simulations and compared with experimental results to authenticate the finite element model. Cutting forces in x-axis and y-axis directions obtained from experiments and simulations have been analyzed and a good agreement is found between them. The resultant cutting forces decrease with the increase in cutting speed. However, with the increase of feed per tooth the resultant cutting forces increase. When the machining is performed along the fiber direction, stresses generated near the tool edge are minimum. The stresses rise with the increase of the fiber cutting angle. This research provides an efficient way to analyze the cutting performance of C_f/SiC composite materials.

Key words: 3D finite element simulation; C_f/SiC composites; milling; cutting force; machinability

CLC number: TG51   **Document code:** A   **Article ID:** 1005-1120(2023)03-0253-11

0 Introduction

Carbon fiber reinforced silicon carbide （C_f/SiC） composite materials are currently applied in many fields of the aerospace industry[1] including leading edge of aircraft, thermal protection systems, and jet engines[2] because of their high thermal stability and mechanical properties[3]. These materials have high strength, excellent wear resistance, high thermal resistance and low density, hence they are replacing conventional materials in various engineering applications[4-5].

Machining of C_f/SiC composites is a difficult job due to their heterogeneity and anisotropy of ceramic matrix which makes them very abrasive. Therefore, processing this composite to get high-efficiency products with the minimum sub-surface damages has become a difficult task that needs to be resolved in modern applications. Numerous researchers have studied the cutting performance of C_f/SiC material. Alaiji et al.[6] observed the chip removal process and analyzed the damage induced in cutting unidirectional carbon fiber reinforced polymer composite material. They have noticed that the damage starts near the cutting edge at the contact point of the tool and chip. Initially, the matrix is cracked and the shearing of fiber-matrix takes place then fiber fracture has occurred. The fiber orienta-

tion angle is very important for chip formation because of the damage between matrix and interface propagates along the direction of fibers[7]. During machining surface roughness at 0° fiber angle is higher as compared to the 90° fiber angle. Pits, cracks and fiber protrusion are the main machined defects at ground surface and side edges[8]. Hu et al.[9] have performed the slot milling process on two-dimensional (2D) C_f/SiC with PCD tool and analyzed the influence of machining parameters on surface roughness, cutting forces, and machined defects. It was observed that resultant cutting forces fluctuated greatly during machining due to rapid changes in fiber cutting angle. Better surface quality can be attained at high cutting speed.

Laser-assisted machining (LAM) is an unconventional machining process used for cutting ceramic matrix composites. Zhao et al.[10] enhanced the machinability of C_f/SiC composites using laser-induced oxidation milling and observed a decrease in surface roughness of about 27.2% as compared to conventional machining process. Liu et al.[11] have observed the decline in average cutting forces of F_x, F_y, and F_z up to 43.7%, 29.16% and 68.09% respectively, when increasing the cutting speed or reducing the feed per tooth and depth of cut during ultrasonic vibration-assisted milling. Zhang et al.[12] studied the failure that occurred in unidirectional (UD) C_f/SiC composites due to the fiber orientation in the grinding process. The fiber fracture and interfacial de-bonding were the main causes of failure. However, the ultrasonic vibration-assisted grinding can reduce the cutting force of about 60% as studied by Wang et al[13].

The feed-rate and cutting speed have large effect on surface roughness of ceramic matrix composites and good surface finish can be achieved by optimizing these parameters[14]. Machining of CMCs is very difficult due to the presence of abrasive fibers which cause various failures in a composite laminate, such as fiber failures, fiber pull-out, delamination, and inter-laminar damage[15]. To find the optimized machining parameters, extensive experimental testings are required. But the high cost of composite materials and cutting tool restrict the number of testings undertaken in this manner.

To solve this problem researchers are using the finite element method (FEM) to analyze the cutting performance of fiber reinforced CMCs. Cepero-mejias et al.[16] have studied the machining of long fiber reinforced polymer (LFRP) composites using FEM. Various techniques such as macro- and micro-scale finite element modeling approaches are being used to investigate the damaged type of composites during machining. Boughdiri et al.[17] have proposed a 3D macro-scale FE model to study the drilling performance of composites and predict the failure in composites such as machining-induced damage and delamination. Micro-scale FE models give good predictions about the damages in material such as matrix cracking, matrix crushing, fiber breakage, and fiber buckling[18]. Macro-scale FE models accurately predict the failure in composites such as machining-induced damage and delamination.

Researchers have studied the cutting performance of C_f/SiC composite materials using milling experiments[9-19]. However, no published literature is found related to the machining performance analysis of C_f/SiC composite material using 3D finite element numerical simulations and its validation with experimental results. This research encompasses the detailed study on the milling performance of C_f/SiC composites at varying machining parameters (i.e., cutting speed, feed per tooth) and material removal mechanisms at different fiber orientations using finite element numerical simulations and experiments.

To achieve this objective, the finite element (FE) model has been created and the slot milling is performed on C_f/SiC composites by using ABAQUS/Explicit computer-aided engineering (CAE) software. Hashin 3D damage criterion is used for fiber failure while Puck and Schurmann damage criterion used for matrix failure[20]. These criteria have been implemented through VUMAT subroutine to get the cutting forces at different machining parameters. Cutting forces from FEA simulations are compared with experimental results to validate the 3D FE model.

1　Experimental Design

C_f/SiC composites composed of T700 carbon fibers and silicon carbide matrix manufactured through chemical vapor infiltration (CVI) is used in this research. The density of the material is about 2.0 g/cm³, the fiber volume fraction is about 35% and the porosity is about 10%. Milling experiments have been conducted on DMU 60 mono BLOCK five-axis CNC machine with a maximum spindle speed of 12 000 r/min. Fig.1 shows the experimental setup.
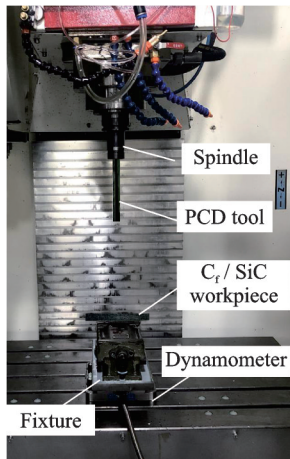

Fig.1　Slot milling experimental setup

A C_f/SiC workpiece with the size of 60 mm × 30 mm × 7 mm has been fixed on a fixture and a two flute straight-edge PCD end mill cutter is used for machining. The physical properties of PCD end mill cutter are given in Table 1. The fixture is clamped with a dynamometer and cutting force values are calculated in x, y and z directions through DynoWare software for 60 s duration. The slot milling operation is performed at different machining parameters like cutting speed and feed per tooth in order to assess the influence of these parameters on cutting forces. Machining parameters used for experiments are presented in Table 2.

2　Finite Element Method (FEM) Simulation

Finite element method is considered as a suitable technique to investigate the cutting performance of ceramic matrix composite materials be-

Table 1　Physical properties of PCD cutter

Parameter	Value
Tool diameter /mm	8
Rake angle /(°)	2
Clearance angle /(°)	9
Edge radius / μm	10
Density / (g·cm⁻³)	4

Table 2　Machining parameters for experiments

Parameter	Value
Cutting speed v_c / (m·min⁻¹)	25, 50, 75
Feed per tooth/mm	0.01, 0.02
Depth of cut/mm	0.2

cause the high cost of CMCs material and cutting tools limit the number of experimental testings. ABAQUS/Explicit is a finite element analysis (FEA) software which gives cost effective alternative, attractive features and independence to perform machining operations like turning, milling, drilling on CMCs by selecting different parameters.

2. 1　Material constitutive model

To perform the slot milling operation on C_f/SiC composites, various modeling approaches (microscale, mesoscale, and macroscale) have been used according to the damage type under consideration in the analysis[21-22]. The microscale modeling approach is used to examine the behavior at the micro level. Both matrix and reinforcements are modeled separately as a deformable continuum. This model helps in assessing the damage type occurring in composite such as fiber buckling, fiber breakage, matrix cracking, and matrix crushing[23]. The macroscale modeling approach is used to examine the behavior of complete structure or laminate and helps in identifying the composite material failure such as delamination and defects occurring during the machining process[24].

Finite element simulation needs to be perfect and reliable to achieve the desired results which are close to the experimental testing. It can predict the forces, failure modes and stresses in the material. In this research, the macroscale FE modeling approach is used to create C_f/SiC composite workpiece and the linear elastic material behavior is as-

sumed before the initiation of damage. The work-piece material is generally modeled by constitutive equations defining the stress-strain response together with its dependence on strain rate and work hardening. Composite materials are considered as orthotropic elastic material as assumed by many researchers[12-26] during finite element analysis. Orthotropic materials are a subgroup of anisotropic materials that show symmetry between two planes[27]. This type of material has three mutually perpendicular symmetry planes at any point in the material. The direction perpendicular to the symmetry planes becomes the elastic principal direction. Within the elastic range, the stress and strain of orthogonal anisotropic composites meet the generalized Hook's law, which is

$$\boldsymbol{\sigma} = \boldsymbol{C}(d) \cdot \boldsymbol{\epsilon} \tag{1}$$

where $C(d)$ is the damaged stiffness matrix and can be expressed as[28]

$$C(d) = \begin{bmatrix} C_{11} & C_{12} & C_{13} & 0 & 0 & 0 \\ C_{12} & C_{22} & C_{23} & 0 & 0 & 0 \\ C_{13} & C_{23} & C_{33} & 0 & 0 & 0 \\ 0 & 0 & 0 & C_{44} & 0 & 0 \\ 0 & 0 & 0 & 0 & C_{55} & 0 \\ 0 & 0 & 0 & 0 & 0 & C_{66} \end{bmatrix} \tag{2}$$

whose non-zero terms can be written as

$$\begin{cases} C_{11} = (1-d_f)E_1(1-\nu_{23}\nu_{32})\Gamma \\ C_{22} = (1-d_f)(1-d_m)E_2(1-\nu_{13}\nu_{31})\Gamma \\ C_{33} = (1-d_f)(1-d_m)E_3(1-\nu_{12}\nu_{21})\Gamma \\ C_{12} = (1-d_f)(1-d_m)E_1(\nu_{21}-\nu_{31}\nu_{23})\Gamma \\ C_{13} = (1-d_f)(1-d_m)E_1(\nu_{31}-\nu_{21}\nu_{32}]\Gamma \\ C_{23} = (1-d_f)(1-d_m)E_2(\nu_{32}-\nu_{12}\nu_{31}]\Gamma \\ C_{44} = (1-d_f)(1-s_{mt}d_{mt})E_1(1-s_{mc}d_{mc})G_{12} \\ C_{55} = (1-d_f)(1-s_{mt}d_{mt})E_1(1-s_{mc}d_{mc})G_{23} \\ C_{66} = (1-d_f)(1-s_{mt}d_{mt})E_1(1-s_{mc}d_{mc})G_{13} \end{cases} \tag{3}$$

where E_i is Young's modulus in the i-direction, G_{ij} the shear modulus in the i-j plane, v_{ij} Poisson's ratio for the transverse strain in the j-direction, and d_f and d_m are the global fiber and matrix damage variables, respectively. The factors S_{mt} and S_{mc} in the definition of shear moduli are introduced to control the reduction of shear stiffness caused by tensile and compressive failures in the matrix. Fiber and matrix damage variables and the constant are also defined as

$$\Gamma = 1/(1-\nu_{12}\nu_{21}-\nu_{23}\nu_{32}-\nu_{13}\nu_{31}-2\nu_{13}\nu_{21}\nu_{32}) \tag{4}$$

$$d_f = 1-(1-d_{ft})(1-d_{fc}) \tag{5}$$

$$d_m = 1-(1-d_{mt})(1-d_{mc}) \tag{6}$$

The elastic constants and strength properties of C_f/SiC composites used to define the material constitutive and damage model are given in Tables 3 and 4[29], respectively.

Table 3   Elastic constants of C_f/SiC composite materials[29]

E_1/ GPa	E_2/ GPa	E_3/ GPa	ν_{12}	ν_{13}	ν_{23}	G_{12}/ GPa	G_{13}/ GPa	G_{23}/ GPa
88.33	61.65	61.65	0.24	0.24	0.33	26.44	26.44	23.17

Table 4   Strength parameters of C_f/SiC composite materials[29]   MPa

Parameter	X_{1t}	X_{1C}	X_{2t}	X_{2C}	S_{12}
Value	235.01	402.57	169.23	317.09	104.72

2.2   Material damage model

To define the damage of composites, various criteria are used by researchers such as Hashin, Hou, Puck, and Tsai-Hill[25]. Hashin failure criterion is widely accepted by researchers to perform FEA of CMCs because of its simple equations. It considers four failure modes for ceramic composites such as tensile fiber failure, fiber compression, matrix cracking, and matrix crushing[29-30]. It was reported that this failure criterion could not predict the matrix failure accurately[20-21]. Hence, the equations related to fiber tension and fiber failure are only used in this analysis, which are stated as

(1) Fiber tension ($\sigma_{11} \geqslant 0$)

$$\left(\frac{\sigma_{11}}{X_{1t}}\right)^2 + \frac{\sigma_{12}^2 + \sigma_{13}^2}{S_{12}^2} \begin{cases} \geqslant 1 & \text{Failure} \\ < 1 & \text{No failure} \end{cases} \tag{7}$$

(2) Fiber compression ($\sigma_{11} < 0$)

$$\left(\frac{\sigma_{11}}{X_{1C}}\right)^2 \begin{cases} \geqslant 1 & \text{Failure} \\ < 1 & \text{No failure} \end{cases} \tag{8}$$

Puck and Schürmann failure criterion has been broadly accepted for predicting the matrix failure[31], which is stated as

(3) Matrix failure

$$\left[\left(\frac{\sigma_{11}}{2X_{1t}}\right)^2 + \frac{\sigma_{22}^2}{|X_{2t} \cdot X_{2C}|} + \left(\frac{\sigma_{12}}{S_{12}}\right)^2\right] + \sigma_{22}\left(\frac{1}{X_{2t}} + \frac{1}{X_{2C}}\right) = 1 \tag{9}$$

where σ_{ij} is the stress components, S_{12} the allowable shear strength, X_{1t}, X_{2t} and X_{2C} are the allowable tensile strength in the fiber and the transverse directions, and compressive strength in the transverse direction, respectively.

2. 3   Model implementation

ABAQUS/Explicit software is used to implement finite element model and the slot milling is carried out on C$_f$/SiC composites. Workpiece is modeled as an orthotropic 3D deformable solid with the size of 8 mm×10 mm×2 mm and a PCD end mill cutter is made as a rigid body because the cutting-edge deformation is not in the scope of this research. User-defined material subroutine has been used to implement material constitutive and damage failure criteria[32]. Performance parameters given in Tables 3 and 4 are entered as mechanical constants in user material section. A flowchart of the model used for the degradation of the material is illustrated in Fig.2.

The FEM simulation of the machining process using material subroutine requires huge calculations due to the involvement of many variables, therefore the time required for completing two rotations of the cutting tool has been fixed for each experimental case. The analysis step defines the output parameters required from numerical simulations, and cut-
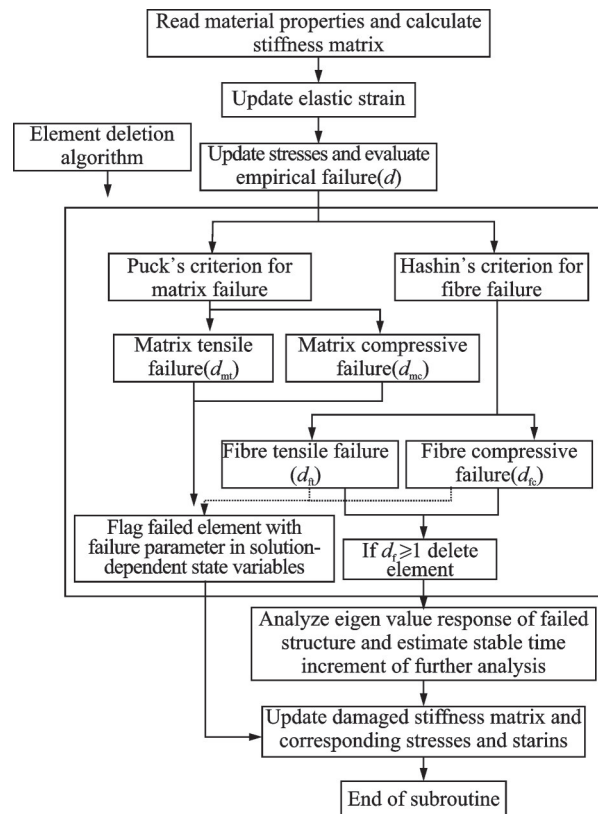

Fig.2   Implementation of VUMAT subroutine[36]

ting forces in x, y and z directions have been selected. The initial step is fixed by default while the dynamic/explicit step is defined to perform the milling operation. The CAD models and assembly of cutting tool and workpiece are shown in Fig.3.
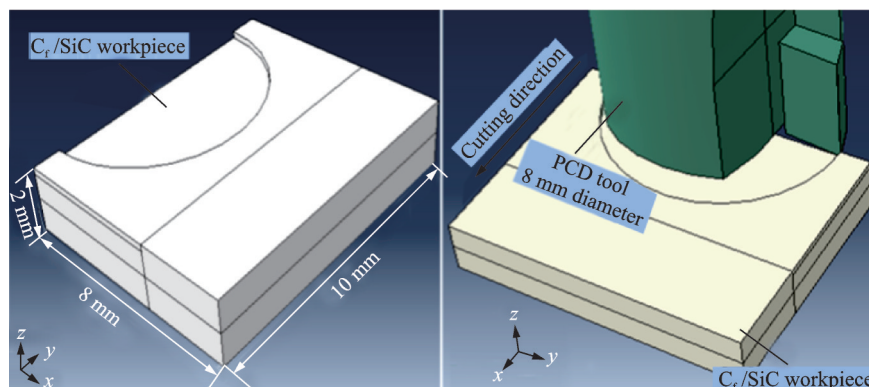

Fig.3   CAD model and assembly of PCD tool and C$_f$/SiC workpiece

Interaction properties determine the contact between the tool and workpiece during the machining process. Both have assigned different surfaces and general explicit contact has been created between them. The cutting tool and the workpiece are defined as master and slave object respectively[26]. The interaction of the workpiece and the tool is of penalty type and hard contact is assumed between them. In the machining process, the friction is an important factor that greatly influences the accuracy of predicting cutting forces during the simulation. The frictional coefficient is taken as a constant value of 0.38

for C_f/SiC materials[33].

The workpiece movements have been restricted in all directions by applying symmetry/encastre boundary conditions. The influence of cutting forces on the tool is not in the scope of this research, therefore milling tool elements have made rigid through a reference point. The velocity/angular velocity boundary condition is used to apply spindle and feedrate at this point. Reduced-integrated 8-node brick elements (C3D8R) element type has been used by various authors[34-35] for composite material which gives three DOFs per node.

The mesh quality greatly affects the efficiency of finite element analysis. To find the appropriate mesh density, various trials of meshes have been conducted with the element size of 0.3, 0.275, 0.25, 0.225 and 0.2 mm at constant cutting speed $v_c = 25$ m/min, depth of cut $a_p = 0.2$ mm and feed per tooth $f_z=0.01$ mm. The mesh convergence is done using resultant cutting forces versus mesh size and the results are nearly the same for 0.2 mm and 0.225 mm mesh density. Therefore, 0.225 mm mesh density has been selected for analysis. To reduce the computational cost, a fine density of mesh is used at the cutting area while a coarse mesh has been used at other regions of workpiece. The element type used for the rigid PCD tool is 4-node linear tetrahedron (C3D4). Finally, the job is created and user defined subroutine file has been chosen as material "input file" and then submitted for analysis. FEM simulations have been conducted according to the machining parameters given in Table 2.

3 Results and Discussion

To validate the numerical finite element model, the comparison of experimental results with simulation results is necessary. The good agreement between them show that the numerical model is validated and can be used to evaluate the behavior of C_f/SiC materials at different machining parameters that is not feasible to achieve through experiments. In this research, the effects of machining parameters on cutting forces have been analyzed including material removal mechanisms in C_f/SiC composites at different fiber orientations.

3.1 Numerical model validation

In FEM cutting simulation, a reference point is fixed on the milling tool at which forces in x and y axis directions are applied during milling process. Forces for the two complete rotations of the tool during the milling of C_f/SiC workpiece have been calculated from both FEA simulation and experiment when the cutting speed v_c is 50 m/min, depth of cut a_p is 0.2 mm and feed per tooth f_z is 0.01 mm as depicted in Figs.4(a) and 4(b). Force profiles created from experiments and simulations are quite similar, which is the evidence that the presented finite element model is validated. The little variations shown in the profiles are due to the presence of factors affecting during conventional machining like heat generation, tool degradation, vibration, porosity, etc.
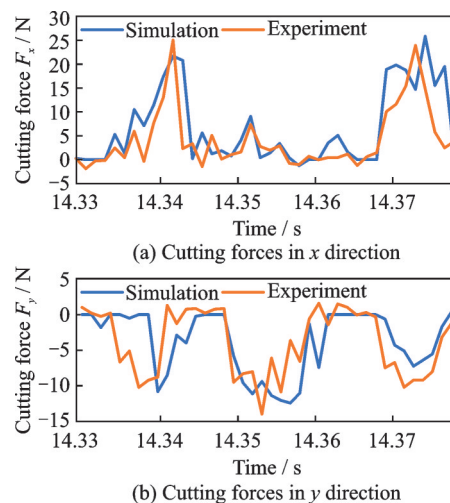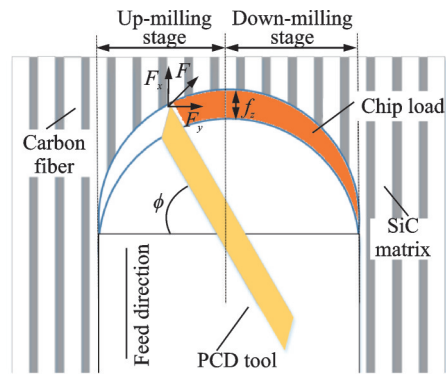

Fig.4 Comparison of cutting forces during milling of C_f/SiC

3.2 Effect of cutting speed on resultant cutting forces

The averaged peak values of resultant cutting forces have been calculated during experiments and FEM simulations at varying cutting speeds. As the tool has two symmetrical edges, the cutting process can be divided in up-milling ($\phi= 0°$ to $90°$) and down-milling ($\phi= 90°$ to $180°$) as shown in Fig.5(a). During the up-milling process, cutting forces increase due to the increase in the thickness of chip formed. When the cutting angle reaches at $90°$, forc-

es are the highest at this point because of the maximum chip thickness and then start decreasing during down-milling process.

(a) Up-milling and down-milling processes
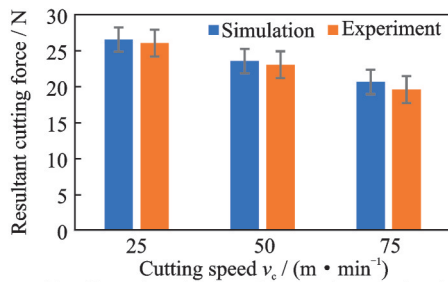
(b) Effect of cutting speed on resultant cutting forces

Fig.5   Effect of cutting speed on resultant cutting force at $f_z = 0.01$ mm and $a_p = 0.20$ mm

Results show that resultant cutting forces decrease with the increase in cutting speeds. At small cutting speed, the un-deformed chip thickness is large, which causes a rise in cutting forces. While with the increasing cutting speed, un-deformed chip decreases and the milling cutter removes the material in plastic mode as the result cutting forces reduce. Fig.5(b) illustrates a graphical comparison of experimental and simulation-based results of average peak values of resultant cutting forces under varying cutting speeds v_c (25—75 m/min) at constant feed per tooth $f_z = 0.01$ mm and the axial depth of cut $a_p = 0.2$ mm. In the milling process, the simulation-based cutting forces are decreased from 28 N to 20.6 N with the increase in cutting speeds. While the decline in cutting forces from 26 N to 19.6 N is observed during experimental results. The change trends of cutting forces in simulated and experimental results are similar and the overall maximum error is found less than 7%. Zhang et al.[19] have also observed the decline in cutting forces from 10.83 N to

2.21 N during conventional milling of 2.5D C_f/SiC composite material at varying spindle speeds of 1 000—2 000 r/min, feed-rate of 25 mm/min and the axial depth of cut of 0.1 mm.

3. 3   Effect of feed per tooth on cutting forces

Fig.6 shows the relationship between the mean value of resultant cutting forces and feed per tooth taken at cutting speed of $v_c = 25$ m/min and depth of cut $a_p = 0.2$ mm. A straight-edge end mill cutter has been used for machining therefore the workpiece and tool edges are perpendicular to each other. For straight-edge end mill cutter, the maximum chip thickness ($f_z = h_{ex}$) is equal to feed per tooth. The increase in feed per tooth increases the chip thickness due to which the material removal load on the tool rises proportionally. With the increase in feed per tooth resultant cutting forces increase accordingly.
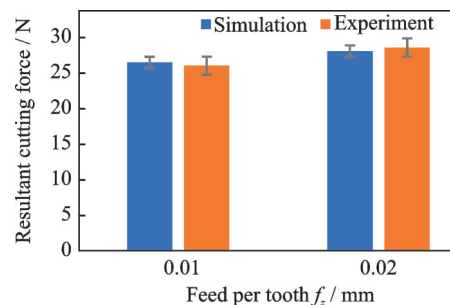

Fig.6   Effect of feed/tooth on resultant cutting forces at $v_c = 25$ m/min and $a_p = 0.20$ mm

3. 4   Material removal mechanism in 0° fiber direction

Results show that the experimental and simulation-based results are similar and an error of about 2% is observed. Resultant cutting forces rise from 26 N to 28 N with the increase in feed per tooth from 0.01 mm to 0.02 mm respectively. Hu et al.[9] have also identified the increase in cutting forces with the rise in feed per tooth during experimental study on milling performance of 2D C/SiC composites using PCD tool. C_f/SiC is anisotropic in nature and the presence of carbon fibers is the dominant factor in increasing cutting forces.
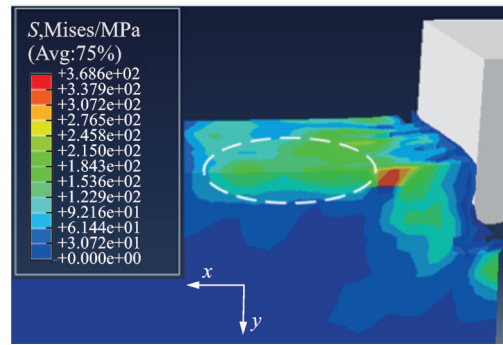
Fig.7 illustrates the material removal mechanism in milling of C_f/SiC at cutting angle $\theta = 0°$

with respect to the fiber direction. When the machining is performed in parallel to the fiber direction, the material is removed mainly due to the debonding of fiber and matrix. Initially, the matrix fracture and crushing of carbon fibers occur near the cutting edge and cracks propagate along the fiber direction. While in the uncut chip area, the bonding of fibers and matrix becomes weak as the fiber axial strength is far stronger than the bonding strength of fibers and matrix, as shown in Fig.7(a).
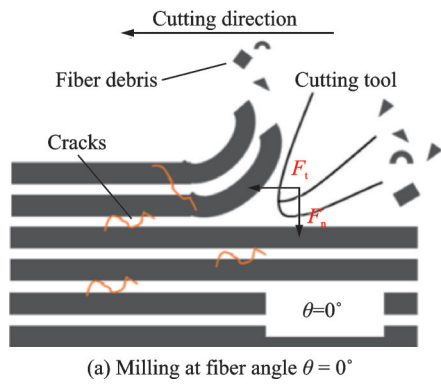
(a) Milling at fiber angle $\theta = 0°$ (b) Numerical simulation of milling at $\theta = 0°$

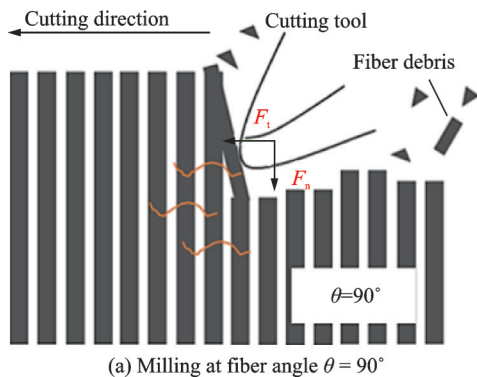Fig.7   Material removal mechanism in milling at 0° fiber direction

Fig.7(b) illustrates the stresss generated in the material during FEM milling of C_f/SiC composites. It is clear from the figure that, stresses mostly occur at the tooltip and propagate along the fiber direction. As the tool moves in the feed direction, brittle cracks form in the SiC matrix, which results in a seperation of fibers from the matrix in the cutting area, while the breakage occurs in the uncut material area as the fibers overcome the axial or shear strength. The debonding of fibers from matrix interface is the main reason of the material deletion, so the cutting stresses are less in this direction.

3.5   Material removal mechanism in 90° fiber direction

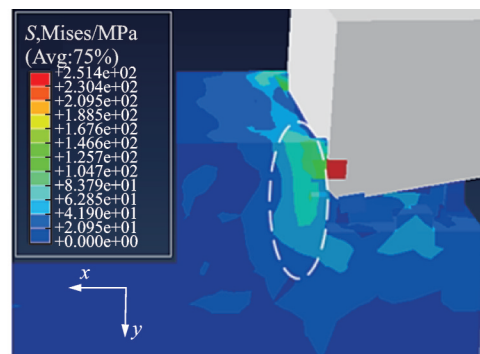Fig.8(a) shows the material removal mechanism at 90° fiber angle. Here, the rake face of the tool is perpendicular to the fiber direction and carbon fibers are subjected to tensile stresses. Initially, cracks occurr ahead of the tooltip and move in the feed direction. The shear strength of fibers is lower than the fiber axial strength. Therefore, when fibers are subjected to the tensile stress they start to elongate and finally break as the force surpasses the fibers shear strength. The friction between the cutting tool and workpiece is maximum at that point and the material has been removed mainly due to the shearing of fiber bundles.

Fig.8(b) illustrates the numerical simulation results when milling performed at $\theta = 90°$ fiber angle. Stresses are mostly distributed at the rake face of cutting tool and the maximum stress is concentrated around the tool edge. When the tool moves forward

(a) Milling at fiber angle $\theta = 90°$ (b) Numerical simulation of milling at $\theta = 90°$

Fig.8   Material removal mechanism in milling at 90° fiber direction

in the feed direction, the carbon fibers stretch and break into pieces because the force exerted by the tool edge exceeds the tensile strength of fibers. Cutting stresses are the sum of tensile and shear stresses of fiber bundles, therefore the maximum stresses are generated in this fiber orientation.

4 Conclusions

The slot milling of C$_f$/SiC composite materials has been performed through 3D finite element analysis simulations using ABAQUS /Explicit solver. The material constitutive and damage model has been implemented through user-defined subroutine. The 3D Hashin failure criterion is used for fiber failure while the Puck and Schurmann failure criterion is used for matrix failure. Then, series of FEM simulations and experiments are performed at different machining parameters to validate the finite element model. The influence of machining parameters (i. e., feed per tooth and cutting speed) on cutting forces has been analyzed along with the material removal mechanism. The following conclusions can be drawn.

(1) Cutting forces in x- and y-axis directions are calculated from both experiments and FEM simulations at cutting speed of 50 m/min, depth of cut 0.2 mm and feed per tooth 0.01 mm. Results have been compared and both cutting forces (F_x and F_y) are found in good agreement as shown in Figs.4(a) and 4(b), validating the finite element model.

(2) Cutting parameters play an important role during machining because they affect the quality of finished product. From experiments, it is evaluated that, at smaller cutting speeds un-deformed chip thickness is large therefore higher cutting forces are needed to detach the material from workpiece, while with the increase in cutting speed material removal load reduces and less cutting forces are required. The increase in feed per tooth also increases the resultant cutting force due to the rise in chip load. Cutting forces are decreased from 28 N to 20.6 N with the increase in cutting speeds from 25 m/min to 75 m/min, while the resultant cutting force rises from 26 N to 28 N with the increase in feed per

tooth from 0.01 mm to 0.02 mm, respectively.

(3) When the machining is performed along the fiber direction ($\theta = 0°$), small stresses are generated only at the tool edge. At this orientation, the material is removed due to the fracture of matrix and crushing of carbon fibers. The debonding of fibers and matrix is the main cause of failure in this direction. When the machining is performed at fiber angle $\theta = 90°$, fibers are subjected to tensile stresses and the material is removed due to the shearing of fiber bundles. Cutting stresses reach the maximum during machining in this orientation.

References

[1] UDAYAKUMAR A, RIZVAN B M, SARABJIT S,et al. Carbon fiber reinforced silicon carbide ceramic matrix composites[M]. [S.l.]: Handbook of Advanced Ceramics and Composites, 2020: 1-35.

[2] ZHANG K, ZHANG L, HE R, et al. Joining of C$_f$/SiC ceramic matrix composites: A review[J]. Advances in Materials Science and Engineering, 2018. DOI: 10.1155/2018/6176054.

[3] XU Z, WANG Y. Study on milling force and surface quality during slot milling of plain-woven CFRP with PCD tools[J]. Materials, 2022, 15(11): 3862.

[4] AN Q, CHEN J, WING W, et al. Machining of SiC ceramic matrix composites: A review[J]. Chinese Journal of Aeronautics, 2021, 34(4): 540-567.

[5] ZHI Fan, ZHANG Ying, SUN Jianbo, et al. A new method for detecting internal defects in composite materials based on time of flight[J]. Transactions of Nanjing University of Aeronautics and Astronautics,2022, 39(3): 314-325.

[6] ALAIJI R E L, LASRI L, BOUAYAD A. 3D finite element modeling of chip formation and induced damage in machining fiber reinforced composites[J]. American Journal of Engineering Research (AJER), 2015, 4(7): 123-132.

[7] VOSS R, SEEHOLZER L, KUSTER F, et al. Influence of fiber orientation, tool geometry and process parameters on surface quality in milling of CFRP[J]. CIRP Journal of Manufacturing Science and Technology, 2017, 18: 75-91.

[8] DU J, ZHANG H, GENG Y, et al. A review on machining of carbon fiber reinforced ceramic matrix composites[J]. Ceramics International, 2019, 45(15): 18155-18166.

[9] HU M, MING W, AN Q, et al. Experimental study on milling performance of 2D C/SiC composites using

polycrystalline diamond tools[J]. Ceramics International, 2019, 45(8): 10581-10588.

[10] ZHAO Guolong, Nian Zhiwen, ZHANG Zhihao, et al. Enhancing the machinability of C_f/SiC composite with the assistance of laser-induced oxidation during milling[J]. Journal of Materials Research and Technology, 2023, 22: 1651-1663.

[11] LIU Yang, LIU Zhibing, WANG Xibin, et al. Experimental study on cutting force and surface quality in ultrasonic vibration-assisted milling of C/SiC composites[J]. The International Journal of Advanced Manufacturing Technology, 2021, 112(7/8): 2003-2014.

[12] ZHANG L, REN C, JI C, et al. Effect of fiber orientations on surface grinding process of unidirectional C/SiC composites[J]. Applied Surface Science, 2016, 366: 424-431.

[13] WANG D, LU S, XU D, et al. Research on material removal mechanism of C/SiC composites in ultrasound vibration-assisted grinding[J]. Materials, 2020, 13(8): 1918.

[14] ZHAO Guolong, XIN Lianjia, LI Liang, et al. Cutting force model and damage formation mechanism in milling of 70wt% Si/Al composite[J]. Chinese Journal of Aeronautics, 2022. DOI: 10.1016/j. cja. 2022.07.018.

[15] LIU C, HOU Z, GAO L, et al. Towards understanding the material removal mechanism in multi-tooth milling of 2.5D C/SiC composites: Numerical modeling and experimental study[J]. The International Journal of Advanced Manufacturing Technology, 2023, 125(9/10): 4163-4184.

[16] CEPERO-MEJÍAS F, CURIEL-SOSA J L, BLÁZQUEZ A, et al. Review of recent developments and induced damage assessment in the modelling of the machining of long fiber reinforced polymer composites[J]. Composite Structures, 2020, 240: 112006.

[17] BOUGHDIRI I, MABROUKI T, ZITOUNE R, et al. 3D macro-mechanical FE simulation for GLARE® drilling with experimental validation[J]. Composite Structures, 2023, 304: 116458.

[18] GARIJO D, MARTÍNEZ F, LOPES C, et al. Multiscale FE modelling and design of composite laminates under impact[J]. Comprehensive Composite Materials II, 2018, 8: 219-238.

[19] ZHANG X, YU T, LI M, et al. Effect of machining parameters on the milling process of 2.5D C/SiC ceramic matrix composites[J]. International Journal of Machining Science and Technology, 2020, 24(2):

227-244.

[20] WANG G D, MELLY S K. Three-dimensional finite element modeling of drilling CFRP composites using Abaqus/CAE: A review[J]. International Journal of Advanced Manufacturing Technology, 2018, 94(1/2/3/4): 599-614.

[21] DANDEKAR C R, SHIN C R. Modeling of machining of composite materials: A review[J]. International Journal of Machine Tools and Manufacture, 2012, 57: 102-121.

[22] CHEN Boyu, YU Hongfa, ZHANG Jinhua. A new 3D meso-mechanical modeling method of coral aggregate concrete considering interface characteristics[J]. Transactions of Nanjing University of Aeronautics and Astronautics, 2022, 39(S): 98-105.

[23] KADDOUR A S, HINTON M J. Maturity of 3D failure criteria for fiber-reinforced composites: Comparison between theories and experiments: Part B of WW-FE-Ⅱ[J]. Journal of Composite Materials, 2013, 47(6/7): 925-966.

[24] ORIFICI A C, HERSZBERG I, THOMSON R S. Review of methodologies for composite material modelling incorporating failure[J]. Composite Structure, 2008, 86(1/2/3): 194-210.

[25] JIANG D, QIAN H, XU Y, et al. Residual strength of C/SiC composite after low-velocity impact[J]. Materials Today Communication, 2022, 30: 103140.

[26] GHAFARIZADEH S, CHATELAIN J F, LEBRUN G. Finite element analysis of surface milling of carbon fiber-reinforced composites[J]. International Journal of Advanced Manufacturing Technology, 2016, 87(1/2/3/4): 399-409.

[27] MÜZEL S D, BONHIN E P, GUIMARÃES N M, et al. Application of the finite element method in the analysis of composite materials: A review[J]. Polymers, 2020, 12(4): 818.

[28] WANG J T, PINEDA E J. 3D progressive damage modeling for laminated composite based on crack band theory and continuum damage mechanics[C]//Proceedings of the 30th Annual Technical Conference of the American Society for Composites. MI, United States: ACS, 2015.

[29] GAO X, YU G, XUE J, et al. Failure analysis of C/SiC composites plate with a hole by the PFA and DIC method[J]. Ceramics International, 2017, 43(6): 5255-5266.

[30] ZHAO L, YANG W, CAO T, et al. A progressive failure analysis of all-C/SiC composite multi-bolt

joints[J]. Composite Structures，2018，202：1059-1068.

[31] PUCK A，SCHÜRMANN H. Failure analysis of FRP laminates by means of physically based phenomenological models[J]. Composites Science and Technology，2002，62(12)：1633-1662.

[32] KHODAEI M，HAGHIGHI-YAZDI M，SAFARABADI M. Numerical modeling of high velocity impact in sandwich panels with honeycomb core and composite skin including composite progressive damage model[J]. Journal of Sandwich Structures and Materials，2020，22(8)：2768-2795.

[33] FAN S，ZHANG L，CHENG L，et al. Microstructure and frictional properties of C/SiC brake materials with sandwich structure[J]. Ceramics International，2011，37(7)：2829-2835.

[34] ANSAR M，XINWEI W，CHOUWEI Z. Modeling strategies of 3D woven composites：A review[J]. Composite Structures，2011，93(8)：1947-1963.

[35] ZHANG P，YAO W，HU X，et al. 3D micromechanical progressive failure simulation for fiber-reinforced composites[J]. Composite Structures，2020，249：112534.

[36] PHADNIS V A，MAKHDUM F，ROY A，et al. Drilling in carbon/epoxy composites：Experimental investigations and finite element implementation[J]. Composites Part A—Applied Science Manufacturing，2013，47(1)：41-51.

Authors   Mr. ELLAHI Zohaib received the B.S. degree in mechanical engineering from Mehran University，Jamshoro，Pakistan，in 2009. From 2009 to 2019，he was employed as a mechanical engineer in engineering and scientific institute，Pakistan. From 2019 to present，he is a postgraduate student in College of Mechanical and Electrical Engineering，Nanjing University of Aeronautics and Astronautics（NUAA）. His research focuses on the machining of carbon fiber reinforced silicon carbide（C$_f$/SiC）ceramic matrix composites.

Prof. **ZHAO Guolong** received his B.S. and Ph.D. degrees of Mechanical Engineering from Shandong University in 2009 and 2015，respectively. Now he is a professor of College of Mechanical and Electrical Engineering in NUAA. His research interests include advanced cutting technology，high performance cutting of composite materials，and micro machining and micro-tool technology.

Author contributions   Mr. **ELLAHI** Zohaib conducted the finite element analysis，interpreted the results and wrote the manuscript. Prof. **ZHAO Guolong** designed the study and experimental setup，provided the guidance in milling experiments and wrote the manuscript. Mr. **NIAN Zhiwen** provided support in the arrangement of machining lab and conducted the experiments. Dr. **MUHAMMAD Jamil** contributed to the analysis of the results. Prof. **HE Ning** supervised the whole research. All authors commented on the manuscript draft and approved the submission.

Competing interests   The authors declare no competing interests.

（Production Editor：WANG Jing）

C$_f$/SiC 复合材料铣削特性的三维有限元分析及试验验证

ELLAHI Zohaib，赵国龙，年智文，MUHAMMAD Jamil，何宁

（南京航空航天大学机电学院,南京210016,中国）

摘要：碳纤维增强碳化硅(C$_f$/SiC)复合材料具有高强度、耐磨损和各向异性等特点,导致材料加工非常困难。本文开展了聚晶金刚石(PCD)刀具铣削C$_f$/SiC复合材料的三维有限元仿真和试验,研究了复合材料的切削特性；研究了加工参数对切削力的影响,以及不同纤维切削角下的材料去除机理。通过用户自定义的子程序在ABAQUS/CAE软件中建立了有限元切削仿真模型,仿真分析了加工参数对切削力的影响,并开展了验证试验。结果表明,有限元仿真和试验得到的 X 和 Y 方向的切削力具有良好的一致性。随着切削速度的增加,切削力降低；随着每齿进给量的增加,切削力升高。当沿着纤维方向进行切削时,刀具刃口的应力最小；随着纤维切削角的增大,刃口应力升高。本文可为C$_f$/SiC复合材料切削特性研究提供指导。

关键词：三维有限元仿真；C$_f$/SiC复合材料；铣削加工；切削力；切削加工性